

Photon storage with sub-nanosecond readout rise time in coupled quantum wells

A.G. Winbow,¹ L.V. Butov,¹ and A.C. Gossard²

¹*Department of Physics, University of California at San Diego, La Jolla, CA 92093-0319*

²*Materials Department, University of California at Santa Barbara,
Santa Barbara, California 93106-5050*

(Dated: July 11, 2008)

Abstract

The following article has been accepted by Journal of Applied Physics. After it is published, it will be found at <http://jap.aip.org/>

Photon storage with 250 ps rise time of the readout optical signal was implemented with indirect excitons in coupled quantum well nanostructures (CQW). The storage and release of photons was controlled by the gate voltage pulse. The transient processes in the CQW were studied by measuring the kinetics of the exciton emission spectra after application of the gate voltage pulse. Strong oscillations of the exciton emission wavelength were observed in the transient regime when the gate voltage pulse was carried over an ordinary wire. Gating the CQW via an impedance-matched broadband transmission line has led to an effective elimination of these transient oscillations and expedient switching of the exciton energy to a required value within a short time, much shorter than the exciton lifetime.

Photon storage is an essential part of optical signal processing in optical networks. Efficient photon storage in semiconductor nanostructures has been recently demonstrated. Photons were stored in the form of separated electrons and holes in acoustically^{1,2} and electrostatically^{3,4,5} induced lateral superlattices, quantum dot pairs,^{6,7,8,9,10} and coupled quantum wells (CQW).¹¹ The fastest demonstrated rise time of the readout optical signal in these devices was about one nanosecond.^{9,11} Here, we report on refining the photon storage in CQW and achieving a 250 ps rise time of the readout optical signal. The refining also has led to an effective elimination of transient oscillations after the storage pulse.

The storage device employs spatially separated electrons and holes in CQW, Fig. 1a. The same device was employed in the proof of principle photon storage in CQW.¹¹ The storage is presented for low temperatures where the spatially separated electrons and holes are bound, forming indirect excitons (for a review on indirect excitons see Ref. 13); however, the operation principle of the device is the same at high temperatures for unbound electrons and holes. The same device and temperature as in Ref. 11 are studied in this paper so that the refined photon storage can be compared with the earlier one.

The principle of the photon storage with CQW is as follows: The emission rate of the indirect excitons (or unbound electrons and holes) is determined by the overlap between the electron and hole wave functions and can be controlled by the applied gate voltage, typically within several orders of magnitude. The energy of the indirect excitons (or unbound pair of electron and hole) is also controlled by the applied gate voltage V_g , which results in the exciton energy shift $\delta E = edF_z$,¹⁴ where d is the separation between the electron and hole layers (close to the distance between the QW centers), $F_z = V_g/D$ is an electric field perpendicular to the QW plane, and D is the width of the intrinsic layer in the $n^+ - i - n^+$ CQW sample. The energy can be typically controlled within several tens of meV in CQW samples. Figs. 2a-d present the schematic of the photon storage. Photons generated by a laser pulse (Fig. 2a) are absorbed in the CQW device. Writing is performed by the gate voltage pulse V_g (Fig. 2b), which reduces the exciton emission rate and stores the absorbed photons in the form of indirect excitons. Emission of the indirect excitons during storage occurs at energy lower by approximately edV_g/D (for corrections due to the interaction see Ref. 13) and is weak due to their long lifetimes. This emission is shown schematically in Fig. 2d. Readout of the stored photons is provided by termination of the gate voltage pulse, which increases the emission rate and results in conversion of excitons back to photons (Fig. 2c). The earlier implementation of this scheme¹¹ demonstrated photon storage with microsecond storage

time and nanosecond rise time of the optical readout.

A principal limitation of the proof-of-principle experimental setup¹¹ was that the gate voltage pulse from the pulse generator was delivered to the CQW sample via ordinary wires over ~ 1 m from the top of the He cryostat to the sample at the bottom. Such a circuit segment is suited for dc signals. However, for the nanosecond switching time of the applied gate voltage, i.e. GHz switching speed, the characteristic wavelength $\sim c/f$ is smaller than the ~ 1 m length of the wire. An impedance-matched broadband transmission line is required in such regime for optimal device performance. This is briefly discussed below.

The characteristic impedance of the pulse generator and external cabling is $Z = 50 \Omega$, while the CQW sample has resistance between the top and bottom planes in the range of $M\Omega - G\Omega$ depending on the laser excitation and acts approximately as a parallel plate capacitor with $C \sim \epsilon S/4\pi D \sim 60$ pF, where $S \sim 0.5 \times 0.5 \text{ mm}^2$ is the sample area. (Note that such circuit also acts as an RC low-pass filter, which slows the switching time.) The apparent impedance mismatch between the ordinary wire and the sample results in reflection of the voltage pulse at the sample and oscillation of the applied voltage V_g and electric field $F_z = V_g/D$ in the sample. We detected these oscillations by analysis of the evolution of the emission spectra, as described below. (The voltage oscillations were also observed on an oscilloscope.) These oscillations hinder the storage in two ways: First, each swing of the oscillating electric field reduces the exciton lifetime and, therefore, reduces the photon storage efficiency. Second, the oscillations complicate the readout process, while waiting for their damping (as in the proof-of-principle experiment)¹¹ sets a minimum storage time.

Furthermore, an ordinary wire also acts as an antenna. In the case when multiple gate voltages are applied to the CQW sample via different wires, the radiation emitted by such an antenna can lead to crosstalk among the wires. Multiple wires are used for creating potential landscapes for excitons, as discussed below, and thus eliminating crosstalk is required for improving the control of potential landscapes for excitons.

Therefore, improving the device performance requires gating the CQW via an impedance-matched broadband transmission line appropriate for the demanded switching speed. In this paper, we exploit gating the CQW sample via a broadband coaxial cable with a 50Ω termination resistor, see Fig. 1b. This method can be applied to a variety of semiconductor structures of diverse layer designs. The achieved performance improvement of our device is described below.

$n^+ - i - n^+$ GaAs/AlGaAs CQW samples were grown by molecular beam epitaxy. The i region consists of a single pair of 8 nm GaAs QWs separated by a 4 nm $\text{Al}_{0.33}\text{Ga}_{0.67}\text{As}$ barrier and surrounded

by 200 nm $\text{Al}_{0.33}\text{Ga}_{0.67}\text{As}$ barrier layers. The n^+ layers are Si-doped GaAs with $N_{\text{Si}} = 5 \times 10^{17} \text{ cm}^{-3}$. The electric field in the sample growth direction F_z is controlled by the gate voltage V_g applied between n^+ layers. At $V_g = 0$, the lowest energy state in the CQW is the direct exciton with a short lifetime, while at $V_g \sim 1.4 \text{ V}$, the lowest energy state is the indirect exciton with a long lifetime, about $0.1 \mu\text{s}$ for the studied sample.

The carriers were photoexcited by a 635 nm laser diode. The 200 ns laser excitation pulse (Fig. 2a) has a rectangular shape with edge sharpness $\sim 0.6 \text{ ns}$ and repetition frequency 500 kHz. The average excitation power was $80 \mu\text{W}$ and the excitation spot diameter was $\sim 100 \mu\text{m}$. The emitted light was diffracted by a single-grating spectrometer and detected by a Peltier-cooled photomultiplier tube and time correlated photon counting system. The experiments were performed in a He cryostat at $T \approx 5 \text{ K}$.

The step-like voltage pulses for the storage and read-out were provided by a pulse generator with 0.5 ns exponential rise/fall time. (Note that the rise time of the readout signal was shorter than 0.5 ns; after termination of the gate voltage pulse, the emission line moves to higher energies to reach the energy at zero electric field and the rise time of the readout optical signal measured at this energy depends on the spectral shape of the emission line and is faster for the lines with a sharp high-energy edge.) The pulse was transmitted within the cryostat over a semi-rigid coaxial cable UT-141B-SS with silver-plated beryllium-copper inner conductor, PTFE teflon dielectric, and stainless-steel outer shell of diameter 3.6 mm, having room-temperature attenuation of 3 dB/m at 10 GHz. The cable bandwidth complies with the requirement for fast control while the cable composition reduces heat conductance to the sample, thus facilitating future measurements with several such cables at low temperatures. The cable was routed vertically straight from the sample through the exterior vacuum SMA feedthrough and countersunk in a channel in the sample plane for good electrical ground. The 5 mm contact pin from the sample socket passed through a hole in the ground plane and terminated on the back side with a metal-film surface-mount resistor having 50Ω at 4.2 K.

Figure 2f shows that the rise time of the readout optical signal in the refined system was 250 ps, which is an improvement compared to the nanosecond rise time achieved in earlier studies.

We also analyzed the transient processes in the CQW after the storage pulse by measuring the kinetics of the exciton emission spectra. Figures 3c,d show the presence of strong oscillations of the exciton emission wavelength in the transient regime for the CQW gated via dc-suited wiring. The oscillation of the emission energy E reveals the oscillation of the electric field in the sample

F_z , with the relation given by $\delta E = ed\delta F_z$. After the voltage pulse, the emission wavelength of the indirect excitons varies from about 810 nm ($E \approx 1.530$ eV) to 793 nm ($E \approx 1.563$ eV), close to the wavelength of the spatially direct emission at 791 nm ($E \approx 1.567$ eV). The emission intensity rises strongly as the wavelength reaches a minimum, caused by the increased recombination rate at smaller F_z ; this causes losses of stored photons.

Figures 3a,b show these oscillations are effectively suppressed when the CQW is gated via an impedance-matched broadband transmission line. After application of the gate voltage pulse, the exciton energy changes without oscillations to the value determined by the applied voltage. The following slow fall in energy observed in Figs. 3a,b is consistent with the reduction of the indirect exciton density with decay, which results in the reduction of the repulsive interaction between the excitons.¹³ The absence of oscillations demonstrates expedient switching at storage. As mentioned above, the oscillations cause losses of stored photons and complicate the readout processes; their elimination improves the device performance. Note that the data reported here demonstrate proof of principle for refining the device performance. The issues essential for practical applications, such as device operation at high temperatures, are briefly discussed in Ref. 11.

We would like to emphasize an important application of the rapid control of the indirect exciton energy and lifetime. A laterally modulated gate voltage $V_g(x, y)$ created by a pattern of electrodes on a sample surface can form a variety of in-plane potential landscapes for indirect excitons in CQW. Particular cases for such potential landscapes include potential gradients,^{15,16} 1D^{3,4,5,17} and 2D¹⁸ lateral superlattices, traps,^{18,19,20,21} and excitonic circuits.²² The switching of the exciton energy to a required value without oscillations and within a short time, much shorter than the exciton lifetime, Figs. 3a,b, demonstrates an improvement for the control of such potential landscapes, which can be exploited in studying the physics of excitons.

Note also that the storage scheme can be used to realize a cold gas of *direct* excitons. Due to their short lifetime, direct excitons are typically hotter than the lattice, while indirect excitons live long enough to cool down essentially to the lattice temperature.¹³ In the storage scheme, initially hot direct excitons transform to indirect excitons by the voltage pulse, cool down toward the lattice temperature during the long storage time, and then transform to direct excitons at the pulse termination. This method uses the long lifetime of indirect excitons to realize a cold gas of direct excitons after the last step, provided that essentially no heating occurs then. Note that indirect excitons have a built-in dipole moment and, therefore, interact relatively strongly.^{23,24,25,26,27} However, direct excitons have no built-in dipole moment and interact weakly. Therefore, this method

may permit extending the studies of cold exciton gases to a new system of weakly interacting cold direct excitons.

In conclusion, gating the CQW via an impedance-matched broadband transmission line has lead to an effective elimination of the transient oscillations in the electric field across the sample and to expedient switching of the exciton energy to a required value within a short time, much shorter than the exciton lifetime. A rise time of the readout optical signal as short as 250 ps was achieved.

This work is supported by ARO, DOE, and NSF. We thank K.L. Campman for growing the high quality samples, and R. Heron, G. Kassabian, B. Naberhuis, and R. Parker for help in preparing the experiment.

-
- ¹ C. Roche, S. Zimmermann, A. Wixforth, J. P. Kotthaus, G. Böhm, and G. Weimann, *Phys. Rev. Lett.* **78**, 4099 (1997).
 - ² P. V. Santos, M. Ramsteiner, and R. Hey, *Phys. Stat. Sol. (b)* **215**, 253 (1999).
 - ³ S. Zimmermann, A. Wixforth, J. P. Kotthaus, W. Wegscheider, and M. Bichler, *Science* **283**, 1292 (1999).
 - ⁴ S. K. Zhang, P. V. Santos, R. Hey, A. Garcia-Cristobal, and A. Cantarero, *Appl. Phys. Lett.* **77**, 4380 (2000).
 - ⁵ J. Krauß, J. P. Kotthaus, A. Wixforth, M. Hanson, D. C. Driscoll, A. C. Gossard, D. Schuh, and M. Bichler, *Appl. Phys. Lett.* **85**, 5830 (2004).
 - ⁶ T. Lundstrom, W. Schoenfeld, H. Lee, and P. M. Petroff, *Science* **286**, 2312 (1999).
 - ⁷ M. Kroutvar, Y. Ducommun, J. J. Finley, M. Bichler, G. Abstreiter, and A. Zrenner, *Appl. Phys. Lett.* **83**, 443 (2003).
 - ⁸ M. Kroutvar, Y. Ducommun, D. Heiss, M. Bichler, D. Schuh, G. Abstreiter, and J. J. Finley, *Nature* **432**, 81 (2004).
 - ⁹ R. J. Young, S. J. Dewhurst, R. M. Stevenson, P. Atkinson, A. J. Bennett, M. B. Ward, K. Cooper, D. A. Ritchie and A. J. Shields, *New J. Phys.* **9**, 365 (2007).
 - ¹⁰ H. J. Krenner, C. E. Pryor, J. He, and P. M. Petroff, arXiv:0805.1819v1.
 - ¹¹ A. G. Winbow, A. T. Hammack, L. V. Butov, and A. C. Gossard, *Nano Lett.* **7**, 1349 (2007).
 - ¹² The term photon storage is used in a general sense and the issue of the carrier or phase information loss is not addressed here.

- ¹³ L. V. Butov, *J. Phys. Condens. Matter* **16**, R1577 (2004).
- ¹⁴ D. A. B. Miller, D. S. Chemla, T. C. Damen, A. C. Gossard, W. Wiegmann, T. H. Wood, and C. A. Burrus, *Phys. Rev. B* **32**, 1043 (1985).
- ¹⁵ M. Hagn, A. Zrenner, G. Böhm, and G. Weimann, *Appl. Phys. Lett.* **67**, 232 (1995).
- ¹⁶ A. Gartner, A. W. Holleitner, J. P. Kotthaus, and D. Schuh, *Appl. Phys. Lett.* **89**, 052108 (2006).
- ¹⁷ S. Zimmermann, A. O. Govorov, W. Hansen, J. P. Kotthaus, M. Bichler, and W. Wegscheider, *Phys. Rev. B* **56**, 13414 (1997).
- ¹⁸ A. T. Hammack, N. A. Gippius, Sen Yang, G. O. Andreev, L. V. Butov, M. Hanson, and A. C. Gossard, *J. Appl. Phys.* **99**, 066104 (2006).
- ¹⁹ T. Huber, A. Zrenner, W. Wegscheider, and M. Bichler, *Phys. Stat. Sol. (a)* **166**, R5 (1998).
- ²⁰ Gang Chen, Ronen Rapaport, L. N. Pfeifer, K. West, P. M. Platzman, Steven Simon, Z. Vörös, and D. Snoke, *Phys. Rev. B* **74**, 045309 (2006).
- ²¹ A. A. High, A. T. Hammack, L. V. Butov, L. Mouchliadis, A. L. Ivanov, M. Hanson, and A. C. Gossard, arXiv:0804.4886v1.
- ²² A. A. High, A. T. Hammack, L. V. Butov, M. Hanson, and A. C. Gossard, *Opt. Lett.* **32**, 2466 (2007).
- ²³ D. Yoshioka and A. H. MacDonald, *J. Phys. Soc. Jpn.* **59**, 4211 (1990).
- ²⁴ X. Zhu, P. B. Littlewood, M. Hybertsen, and T. Rice, *Phys. Rev. Lett.* **74**, 1633 (1995).
- ²⁵ Yu. E. Lozovik and O. L. Berman, *JETP Lett.* **64**, 573 (1996).
- ²⁶ A. L. Ivanov, *Europhys. Lett.* **59**, 586 (2002).
- ²⁷ C. Schindler and R. Zimmermann, arXiv:0802.3337.

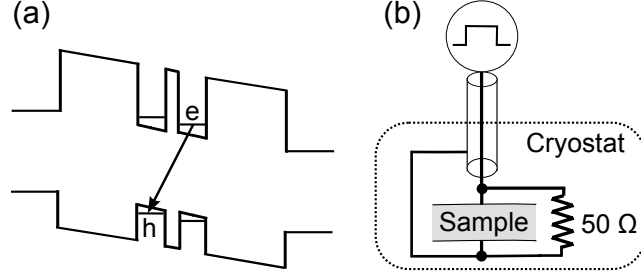


FIG. 1: (a) GaAs/AlGaAs CQW band diagram. (b) Schematic of the photon storage circuit with an impedance-matched broadband transmission line.

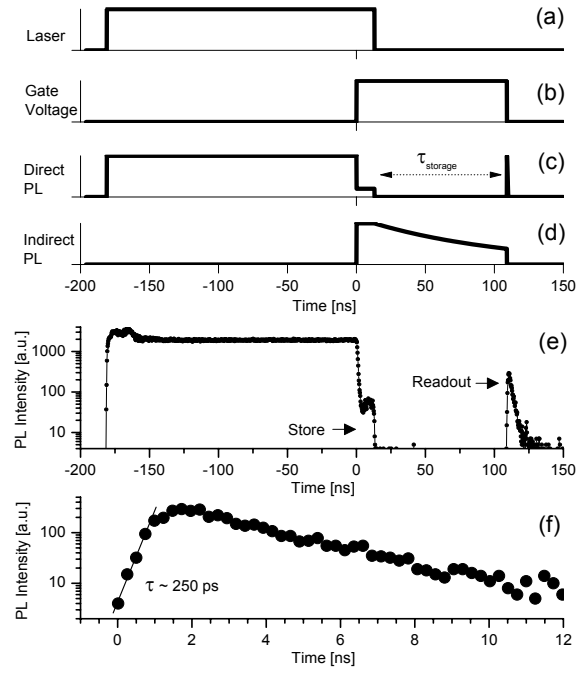


FIG. 2: (a)–(d) Schematic of the photon storage and readout in the CQW device showing the sequence of the laser (a) and gate voltage (b) pulses as well as the emission of direct (c) and indirect (d) excitons. The operation principle of the device is described in the text. (e,f) Experimental implementation of the photon storage in the CQW device. The gate voltage pulse $V_g = 1.4$ V. (e) Kinetics of the direct exciton emission of the refined system with an impedance-matched broadband transmission line, demonstrating photon storage followed by readout. The timescale on the schematic (a-d) corresponds to the experimental data. (f) The readout pulse on an extended time scale. The exponential fit (line) gives the rise time $\tau_{\text{readout}} \sim 250$ ps. The fall time and FWHM of the readout signal are both 2.5 ns.

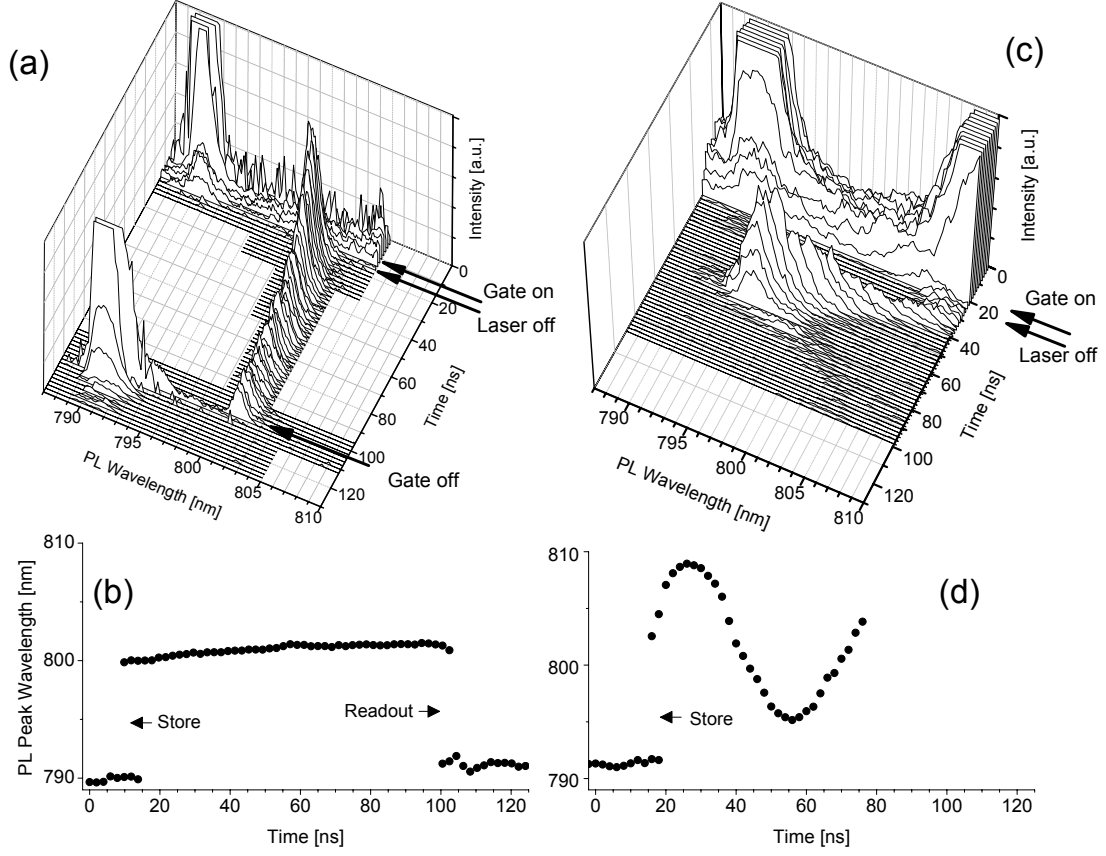


FIG. 3: Evolution of emission spectra during storage and readout for (a,b) the refined system employing an impedance-matched broadband transmission line and (c,d) the proof-of-principle system employing dc-suitied wiring. The applied voltage is $V_g = 1.4$ V. Each spectrum is stepped 2 ns apart in time and is measured within a 2.3 ns window. The emission peaks while the laser is on (a,c) and at readout (a) are clipped in the plots to show small scale details. In the proof-of-principle system, the readout PL pulse occurs later in time and is not shown. Bulk n^+ PL is seen at $\lambda \gtrsim 805$ nm during the laser pulse in (c). (b,d) The mean emission peak wavelength $\bar{\lambda}_{\text{peak}} = \int \lambda I(\lambda) d\lambda / \int I(\lambda) d\lambda$ for the spectra presented in (a,c). The refined system eliminates the emission oscillations suffered by the proof-of-principle system after the voltage pulse.